

SCAP: Transductive Test-Time Adaptation via Supportive Clique-based Attribute Prompting

Chenyu Zhang*, Kunlun Xu*, Zichen Liu, Yuxin Peng, Jiahuan Zhou†

Wangxuan Institute of Computer Technology, Peking University, Beijing 100871, China

{2200010814, xkl, lzc20180720}@stu.pku.edu.cn, {pengyuxin, jiahuanzhou}@pku.edu.cn

Abstract

Vision-language models (VLMs) encounter considerable challenges when adapting to domain shifts stemming from changes in data distribution. Test-time adaptation (TTA) has emerged as a promising approach to enhance VLM performance under such conditions. In practice, test data often arrives in batches, leading to increasing interest in the transductive TTA setting. However, existing TTA methods primarily focus on individual test samples, overlooking crucial cross-sample correlations within a batch. While recent ViT-based TTA methods have introduced batch-level adaptation, they remain suboptimal for VLMs due to inadequate integration of the text modality. To address these limitations, we propose a novel transductive TTA framework, Supportive Clique-based Attribute Prompting (SCAP), which effectively combines visual and textual information to enhance adaptation by generating fine-grained attribute prompts across test batches. SCAP first forms supportive cliques of test samples in an unsupervised manner based on visual similarity and learns an attribute prompt for each clique, capturing shared attributes critical for adaptation. For each test sample, SCAP aggregates attribute prompts from its associated cliques, providing enriched contextual information. To ensure adaptability over time, we incorporate a retention module that dynamically updates attribute prompts and their associated attributes as new data arrives. Comprehensive experiments across multiple benchmarks demonstrate that SCAP outperforms existing state-of-the-art methods, significantly advancing VLM generalization under domain shifts. Our code is available at <https://github.com/zhoujiahuan1991/CVPR2025-SCAP>.

1. Introduction

Vision-language models (VLMs) such as CLIP [32] have exhibited remarkable generalization capabilities across a

*Equal contribution

†Corresponding author

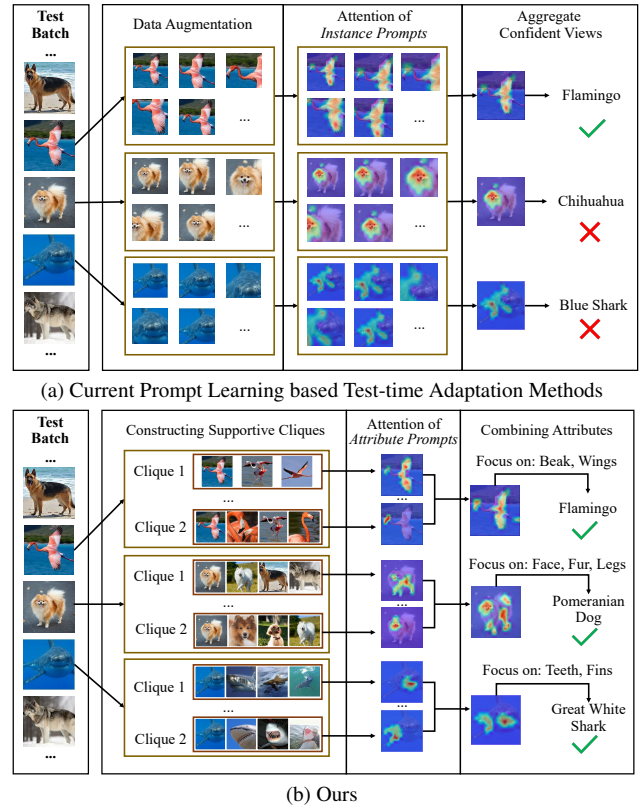


Figure 1. Comparison between our proposed SCAP to existing prompt learning-based TTA methods. Specifically, current TTA methods learn from instances, while our method utilizes cross-sample visual similarity information from batches to construct *supportive cliques* and extract *attributes* from them. We learn attributes from both modalities based on the cliques. For each image, SCAP jointly utilizes attribute prompts from its associated cliques, leading to more effective and accurate prompting.

training distribution [10, 36, 44, 54]. This limitation has sparked increasing interest in the area of *Test-Time Adaptation (TTA)* [1, 2, 39, 49], which aims to adapt pre-trained VLMs to mitigate domain shifts during test time.

Recent works in TTA have primarily focused on adapting CLIP by independently learning from each sample during test time [20, 25, 36, 49]. However, in real-world scenarios, test-time data typically arrives in batches, creating a *transductive TTA setting*. Existing TTA methods can tackle such a scenario by treating each test sample individually [25]. Although this solution is available, it suffers from significant limitations due to disregarding the intrinsic cross-sample visual similarity within each batch. Exploiting these inter-sample similarities can greatly enhance both the effectiveness and robustness of the adaptation process. As illustrated in Figure 1, test batches often contain *Cliques*, groups of visually and semantically similar images that share common characteristics, referred to as *Attributes* in this paper. Leveraging these cliques enables a more precise and context-aware adaptation by guiding the model to focus on discriminative attributes.

Recent works [13, 17, 28, 31, 38] have explored transductive TTA under the Vision Transformer (ViT) backbone, often relying on batch statistics to adjust normalization parameters or select class-balanced samples for adaptation. However, these methods cannot be directly applied to CLIP since they completely neglect the adaptation of the text modality, which is crucial in VLMs. Rare CLIP-based TTA methods are designed for the transductive setting. In the latest method [14], the top-k predicted classes of each image in a batch are aggregated into a single new text prompt, which is used as pseudo labels to reclassify inputs in a transductive manner. However, the aforementioned transductive TTA methods mainly perform coarse-grained batch-level utilization of the visual similarity information. Thus, the fine-grained discriminative attribute information of cross-sample visual similarity is underutilized.

In this paper, we propose *Supportive Clique-based Attribute Prompting (SCAP)*, a novel CLIP-based transductive TTA approach designed to effectively leverage the cross-sample visual similarity information. Given a test batch, SCAP automatically mines distinct *Supportive Cliques* containing test images with shared attributes by leveraging visual and semantic similarity metrics. These cliques play a crucial role in learning *Attribute Prompts* that capture discriminative, attribute-specific information for each clique. For any given test sample, its aggregated attribute representation is constructed by combining the learned attribute prompts associated with the cliques to which it belongs. By utilizing these aggregated attribute prompts, SCAP enables CLIP to focus on fine-grained, instance-specific details, enhancing prediction accuracy and robustness. Additionally, we introduce a retention mechanism that dynamically up-

dates and preserves attribute prompts, ensuring long-term adaptability across tasks. Extensive experiments on two benchmarks demonstrate that SCAP significantly outperforms various current state-of-the-art methods in the transductive TTA setting, showing the effectiveness of SCAP in mining the intrinsic knowledge in batches.

In summary, the contributions of this work are four-fold: (1) We propose Supportive Clique-based Prompting (SCAP), a novel approach that leverages the rich information of cross-sample relationships, improving the effectiveness of test-time adaptation under *transductive setting*. (2) To achieve robust and accurate fine-grained attribute prompt learning during test time, we propose to learn attribute prompts in a transductive manner based on cliques. (3) To retain the historically learned attribute prompts, we further design a retention mechanism to preserve the learned prompts for future reuse. (4) Extensive experiments on two benchmarks demonstrate that SCAP outperforms several current state-of-the-art methods in the transductive TTA setting, highlighting its effectiveness in extracting intrinsic knowledge from batches.

2. Related Work

2.1. Prompt Learning for CLIP

VLMs like CLIP have demonstrated abundant knowledge learned from large-scale image-text data [5, 18, 19, 32, 33, 45]. Adapting CLIP to various downstream tasks is a valuable and challenging problem [3]. Recently, prompt learning [23, 24, 37, 48, 51] has emerged as a promising approach for enhancing model adaptability. Specifically, CoOp [57], CoCoOp [56], MaPLe [21], and Tip-Adapter [51] have achieved state-of-the-art performance. However, they rely on training data from downstream tasks. However, these approaches rely on training data annotations and often struggle when faced with substantial domain shifts at test time [38, 42].

2.2. Test-Time Adaptation

Test-time adaptation (TTA) focuses on dynamically adjusting pre-trained models, such as CLIP or ViTs [22, 25], by leveraging sequentially obtained unlabeled test data [9, 11, 38, 49, 50]. Existing TTA approaches can be broadly categorized into training-free, augmentation-based, and prompt-based methods. Training-free methods aim to adapt CLIP efficiently without backpropagation [7, 20]. TDA introduces a positive and negative cache mechanism to assist prediction. Zero [7] aggregates predictions from multiple augmented versions without modifying model parameters. The augmentation-based methods [6, 49] focus on generating diverse augmented samples to integrate test distribution knowledge into the model. MTA [49] introduces a quality assessment variable for each

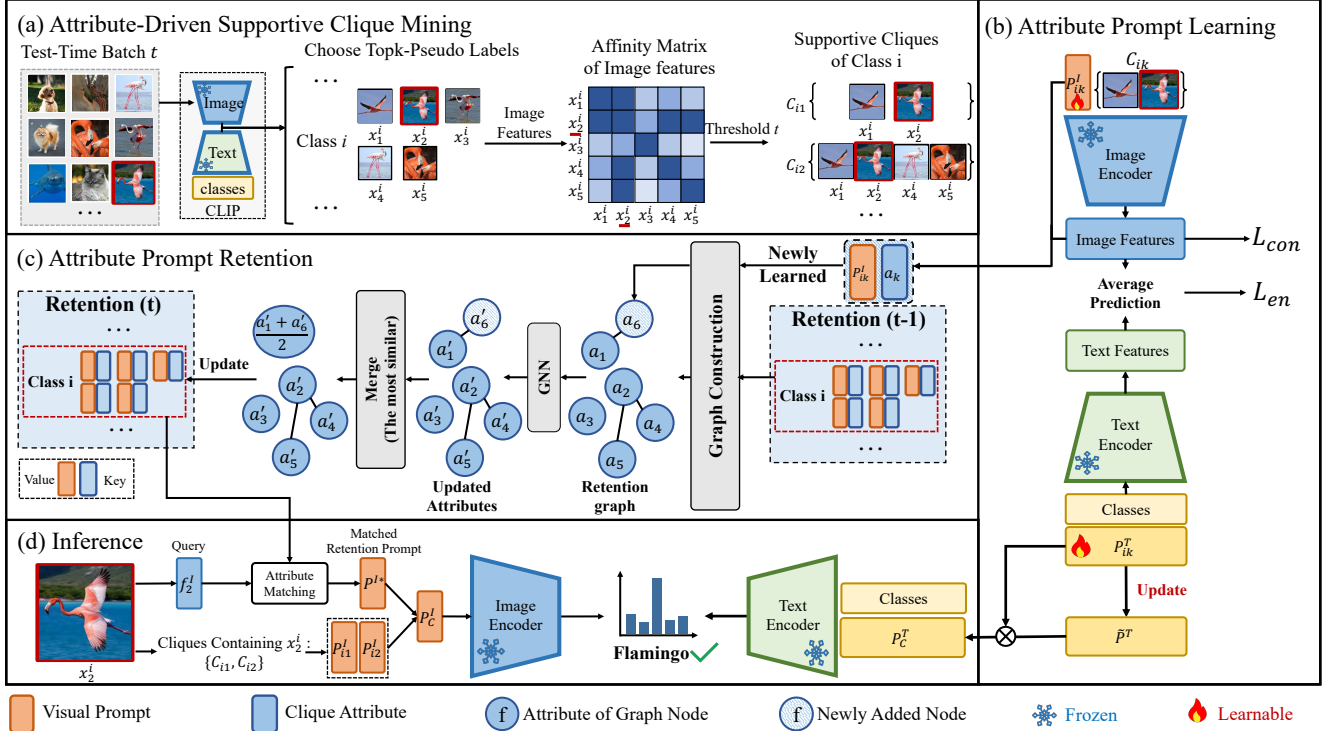


Figure 2. Overview of our proposed SCAP. SCAP firstly mines the *supportive cliques* for all images in parallel. Based on the cliques, it then learns the corresponding *attribute prompts* from both modalities. The learned *visual attribute prompts* and the *text attribute prompts* are separately retained to accumulate the knowledge of test domains. For each instance, we conduct inference by jointly utilizing all the associated attribute prompts and the retained knowledge to generate the final prediction.

augmented view and models the distribution using a mixed Gaussian approach. Prompt-based methods employ prompt tuning to adapt the model while preserving generalization capabilities [12, 25, 26, 36, 47, 50]. For example, TPT [36] optimizes instance-specific text prompts by minimizing prediction entropy, whereas DART [25] refines prompts across both modalities while leveraging historically learned knowledge via prompt retention. While these methods assume a sequential data setting where test samples are processed individually [13, 38], real-world scenarios often involve test-time data arriving in batches. Consequently, existing approaches struggle to exploit the inter-sample relationships within a batch, leading to suboptimal adaptation performance.

2.3. Transductive Test-Time Adaptation

Transductive TTA considers the practical scenario where test data are provided in batches rather than individual samples. Existing Transductive TTA methods are predominantly developed for ViTs pre-trained on ImageNet [13, 28, 31, 35, 39, 41]. These approaches typically rely on batch statistics to update normalization parameters [39] or select confident samples for model tuning [28]. Recent studies have demonstrated that CLIP outperforms ViTs pre-trained

on ImageNet in TTA tasks. However, existing transductive TTA methods fail to fully exploit CLIP’s capabilities, as they largely disregard the adaptation of the text modality, which is crucial for leveraging its knowledge learned from vision-language alignment. A few recent efforts have attempted to adapt CLIP for transductive TTA. For example, CLIPArTT [14] optimizes the model by jointly utilizing all images within a batch. However, since cross-instance relationships within a batch are often imbalanced, directly modeling all samples together does not effectively exploit the most informative relationships. In this work, we take a step further by identifying and leveraging the informative cliques, groups of strongly correlated samples within a batch, to facilitate robust adaptation by capturing discriminative attributes.

3. Method

3.1. Problem Setting and Notations

In transductive TTA, test data arrive sequentially in batches. Given t -th test batch $B_t = \{x_j\}_{j=1}^b$, where b is the batch size and x_j is a test image. We generate a set of Supportive Cliques for each class i , denoted as $C_i = \{C_{ik}\}_{k=1}^m$. Then, we extract the corresponding clique attributes, which are de-

noted as $\mathcal{A}_i = \{a_{ik} \in \mathbb{R}^d\}_{k=1}^m$ where d is the attribute dimension, equivalent to the feature dimension. Additionally, we introduce Attribute Prompts $\mathcal{P}_i^A = \{\mathcal{P}_i^I, \mathcal{P}_i^T\}$, which consist of visual attribute prompts $\mathcal{P}_i^I = \{P_{ik}^I\}_{k=1}^m$ and text attribute prompts $\mathcal{P}_i^T = \{P_{ik}^T\}_{k=1}^m$. Our model θ is built on CLIP, which comprises an image encoder \mathbf{E}_I and a text encoder \mathbf{E}_T .

3.2. Attribute-Driven Supportive Clique Mining

Attributes are the fine-grained characteristics shared by a group of images in the batch. Since images containing the same attribute often exhibit high visual similarity to each other, in this section, we propose to obtain Supportive Cliques for the potential attributes by evaluating cross-image similarity.

Specifically, we use CLIP to obtain the top- k class predictions $topk(x_j)$ for each image x_j , where k is a hyperparameter. For each class i , all images whose top- k predictions include class i are selected to form a subset S_i :

$$S_i = \{x_j \in B_t : i \in topk(x_j)\} \quad (1)$$

Since images in S_i share similar class-specific information, which ensures semantic relevance. To further capture more fine-grained relevance, we extract the features $F_i^I \in \mathbb{R}^{|S_i| \times d}$ of images within S_i using the CLIP image encoder \mathbf{E}_I and compute the similarity matrix $M_i \in \mathbb{R}^{|S_i| \times |S_i|}$ as follows:

$$M_i = F_i^I \cdot (F_i^I)^\top \quad (2)$$

Then, given the l -th row of M_i , we collect elements exceeding a threshold t , whose corresponding images form a Clique C_{il} . Formally, the Clique generated from the l -th row of M_i is defined as:

$$C_{il} = \{x_j^i : x_j^i \in S_i, (M_i)_{lj} > t\}, \quad (3)$$

where $(M_i)_{lj}$ represents the l -th row, j -th column of M_i . Only non-trivial Cliques ($|C_{il}| > 1$) are retained, and duplicate Cliques are removed to ensure uniqueness. Finally, we obtain a set of valid Cliques $\mathcal{C}_i = \{C_{ik}\}_{k=1}^m$.

3.3. Attribute Prompt Learning

In this section, we aim to learn prompts that capture attribute-specific knowledge to facilitate classification.

Specifically, for each Clique C_{ik} , we learn a visual attribute prompt P_{ik}^A from the image modality and a text attribute prompt P_{ik}^T from the text modality. The feature $f_j^I \in \mathbb{R}^d$ for the j -th image in C_{ik} is extracted as:

$$f_j^I = \mathbf{E}_I(C_{ik}^j, P_k^I) \quad (4)$$

Then, we define the attribute feature $a_{ik} \in \mathbb{R}^d$ of C_{ik} which is calculated by:

$$a_{ik} = \frac{1}{|C_{ik}|} \sum_{j=1}^{|C_{ik}|} f_j^I \quad (5)$$

Besides, we compute the text feature f_n^T of the n -th class as follows:

$$f_n^T = \mathbf{E}_T(c_n, P_{ik}^T) \quad (6)$$

Given total N classes, we introduce an attribute-specific class probability distribution vector, which is obtained by:

$$\hat{\mathbf{P}}_{ik} = [\hat{p}_{ik}^1, \hat{p}_{ik}^2, \dots, \hat{p}_{ik}^N] \quad (7)$$

where

$$\hat{p}_{ik}^n = \frac{\exp(\cos(a_{ik}, f_n^T)/\tau)}{\sum_{j=1}^N \exp(\cos(a_{ik}, f_j^T)/\tau)} \quad (8)$$

Note that $\cos(\cdot, \cdot)$ denotes cosine similarity and τ is a temperature parameter to scale the similarity scores.

Then, we compute the *Entropy Loss* for the probability distribution of the attribute:

$$\mathcal{L}_{en}(C_{ik}) = - \sum_{n=1}^N \hat{p}_{ik}^n \log \hat{p}_{ik}^n \quad (9)$$

To further guide the model to extract attribute-specific information and discard attribute-irrelevant information, we introduce a concentration loss $\mathcal{L}_{con}(C_{ik})$ that forces the model to capture the shared information across the samples within a Clique. Specifically, $\mathcal{L}_{con}(C_{ik})$ is calculated by

$$\mathcal{L}_{con}(C_{ik}) = \sum_{j=1}^{|C_{ik}|} \|f_j^I - a_{ik}\|^2 \quad (10)$$

Therefore, both kinds of prompts P_{ik}^I and P_{ik}^T are guided to encode attribute-specific knowledge as the model optimization. Such knowledge is valuable when generating predictions for images showing the same attributes.

3.4. Attribute Prompt Retention

In this section, to retain attribute knowledge during the test process and ensure consistent performance improvement, we introduce mechanisms for retaining both text and visual attribute knowledge.

Firstly, to retain the text attribute knowledge, we propose a *Text Retention Prompt* \tilde{P}^T . Specifically, when a new Clique C_{ik} is learned, we update \tilde{P}^T by

$$\tilde{P}^T = \alpha_\tau \tilde{P}^T + (1 - \alpha_\tau) P_{ik}^T, \quad (11)$$

where $\alpha_\tau = \tau/(1 + \tau)$ is a decay rate based on iteration count τ .

Besides, to retain the visual attribute knowledge, we design a *Retention Cache* $\mathcal{R} = \{R_i\}_{i=1}^N$ where R_i is a class-specific retention cache. Specifically, we store (a_{ik}, P_{ik}^I) as key-value pairs in R_i . We denote the retained attributes (*i.e.* keys) as $R_i^A = \{a_1, \dots, a_L\}$ and the corresponding attribute prompts (*i.e.* values) as $R_i^P = \{P_1^I, \dots, P_L^I\}$. The

maximum size of each R_i is set to L to avoid memory explosion. When the retained key-value pair number is less than L , we directly add a new (a_{ik}, P_{ik}^I) to R_i . Otherwise, we add (a_{ik}, P_{ik}^I) to R_i first, then we update all pairs and aggregate the two that are most similar to each other in R_i by using a graph structure as follows.

Firstly, we construct a weighted graph $G_i = (V_i, E_i)$. The vertices are the keys in the retention cache $V_i = R_i^A = \{a_1, \dots, a_{L+1}\}$. The edges E_i between each two vertices are defined as the Gaussian Distance of the two attributes. Thus, the adjacency matrix $W_i \in \mathbb{R}^{(L+1) \times (L+1)}$ of G_i is defined with:

$$(W_i)_{kl} = \exp\left(-\frac{\|a_k - a_l\|^2}{2\sigma^2}\right), \quad (12)$$

where $(W_i)_{kl}$ is the k -th row, l -column of W_i and σ is a hyperparameter. We utilize the K -max values in each row of W_i to construct a K -nearest retention graph. Then we perform graph propagation following [53] and obtain the *updated* graph vertices $V'_i = \{a'_{j_0}, \dots, a'_{j_1}\}$, where the similar attributes are pushed closer automatically. Then, the most similar two attributes a'_{j_0}, a'_{j_1} and the corresponding prompts are fused into one respectively as follows:

$$\begin{cases} a_{new} = \frac{1}{2}(a'_{j_0} + a'_{j_1}) \\ P_{new}^I = \frac{1}{2}(P_{j_0}^I + P_{j_1}^I) \end{cases} \quad (13)$$

Through the above process, we obtain the *updated* retention cache R_i , dynamically retaining the visual and text attribute knowledge learned from previous batches into *Retention Cache* and *Text Retention Prompt*, respectively.

3.5. Optimization and Inference

For each batch B_t , we optimize the visual attribute prompts $\mathcal{P}_i^I = \{P_{ik}^I\}_{k=1}^m$ and text attribute prompts $\mathcal{P}_i^T = \{P_{ik}^T\}_{k=1}^m$ for every class i by minimizing the following loss function:

$$\mathcal{L} = \sum_{k=1}^m \mathcal{L}_{en}(C_{ik}) + \lambda \mathcal{L}_{con}(C_{ik}) \quad (14)$$

where λ is a hyperparameter.

Then we conduct inference for each S_i of B_t . To fully utilize both the *Attribute Prompts* learned from the current batch B_t and the *retained knowledge* to improve prediction. Given the test image $x_j \in S_i$, we first collect all Cliques containing x_j , namely $\mathcal{K} = \{k : x_j \in C_{ik}\}$, whose corresponding visual attribute prompts are concatenated together:

$$P^I = \text{concat}(\{P_{ik}^I : k \in \mathcal{K}\}) \quad (15)$$

Then, we introduce the retention prompt matching strategy utilizing the key-value pair structure of the retention

cache. Specifically, the keys are the retained attribute features $R_i^A = \{a_1, \dots, a_L\}$ and the values are the corresponding attribute prompts $R_i^P = \{P_1^I, \dots, P_L^I\}$. Given the image feature f_j^I of x_j which is already extracted in Sec. 3.3, the top-1 attribute a^* is obtained by evaluating the similarity of f_j^I to all keys in R_i^A , *i.e.*

$$a^* = \operatorname{argmax}_{a_l \in R_i^A} \langle f_j^I, a_l \rangle \quad (16)$$

Given the matched value corresponding to a^* , *i.e.*, P^{I^*} , we obtain the *Composed Image Prompt* P_C^I by concatenating P^I and P^{I^*} along the token dimension

$$P_C^I = \text{concat}(P^I, P^{I^*}) \quad (17)$$

For the text modality, we fuse $\mathcal{P}^T = \{P_{ik}^T\}_{k=1}^m$ and \tilde{P}^T together to get the *Composed Text Prompt* P_C^T :

$$P_C^T = \alpha_r \tilde{P}^T + (1 - \alpha_r) \frac{1}{m} \sum_{k=1}^m P_{ik}^T \quad (18)$$

where α_r is the weight of retained text prompts. Then, for the final prediction, the image-inference feature \hat{f}_j^I of x_j and the text-inference feature \hat{f}_n^T of class c_n are obtained by:

$$\begin{cases} \hat{f}_j^I = \mathbf{E}_I(x_j, P_C^I) \\ \hat{f}_n^T = \mathbf{E}_T(c_n, P_C^T) \end{cases} \quad (19)$$

The prediction y_j of x_j is obtained by applying Eq.7.

4. Experiments

In this section, we first introduce the two benchmarks used for model evaluation, followed by a detailed description of the implementation setup. Next, we present a comparative analysis of existing methods and our proposed approach. Finally, extensive ablation studies are conducted to validate the effectiveness of SCAP. Additional experimental results and in-depth discussions are provided in the Supplementary Materials.

4.1. Benchmarks

Our evaluation is conducted on two benchmarks: an out-of-distribution (OOD) benchmark and a cross-domain benchmark. The OOD benchmark consists of four datasets derived from ImageNet [4], *i.e.*, ImageNet-A [16], ImageNet-R [15], ImageNet-Sketch [40], and ImageNet-V2 [34]. The OOD benchmark aims to assess the model's robustness to substantial distribution shifts in the test data. The cross-domain benchmark comprises four datasets of the image classification task, each representing a distinct domain: Aircraft [27], Caltech101 [8], Flower102 [29], and Pets [30]. The cross-domain benchmark provides a measure of the model's adaptability across a diverse range of domain-specific tasks.

Method	Publication	ImageNet-A	ImageNet-R	ImageNet-S	ImageNet-V2	Average
CLIP [32]	ICML 2021	47.87	73.98	46.09	61.88	57.46
CoOp [57]	IJCV 2022	49.71	75.21	47.99	64.20	59.28
CoCoOp [56]	CVPR 2022	50.63	76.18	48.75	64.07	59.91
Tip-Adapter [51]	ECCV 2022	51.04	77.76	48.88	63.41	60.27
TPT [36]	NeurIPS 2022	54.77	77.06	47.94	63.45	60.81
C-TPT [47]	ICLR 2024	52.90	78.00	48.50	63.40	60.70
DART [25]	AAAI 2024	60.56	79.56	49.76	64.03	63.48
MTA [49]	CVPR 2024	58.06	78.33	49.61	64.24	62.56
TDA [20]	CVPR 2024	60.11	80.24	50.54	64.67	63.89
Zero [7]	NeuIPS 2024	61.35	77.28	48.29	64.13	62.76
SCAP	This Paper	64.52	81.68	51.65	64.65	65.63

Table 1. **Results comparison on the out-of-distribution (OOD) Benchmark.** The results of the compared methods follow the original paper or are implemented with the official code [25].

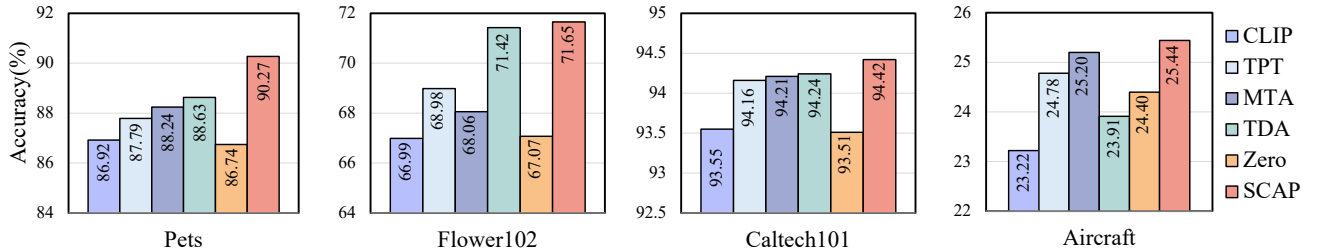


Figure 3. **Results on the Cross-Domain Benchmark.** Comparison of SCAP with state-of-the-art methods. All methods are evaluated using CLIP-ViT-B/16 as the backbone.

Implementation details. We adopt CLIP with ViT-B/16 as the backbone and set the batch size to 64 for all experiments. Visual attribute prompts are initialized using a uniform distribution in the range $(-1, 1)$, following previous TTA methods [25, 36]. For text attribute prompts, we employ an ensemble of multiple templates for the OOD benchmark, whereas dataset-specific templates are used for the cross-domain benchmark, following TDA [20]. Our key hyperparameters include the threshold t for supportive clique extraction, the weight α_r for computing P_C^T , the concentration loss weight λ , and graph structure parameters σ , L , and K . The hyperparameter ablations of this paper are conducted on ImageNet-A, with the default values of α_r , σ , L , and K set to 1, 0.3, 6, and 3, respectively. We set $k = 3$ in the initial top-k predictions Eq. (1). An Adam optimizer with a learning rate of 0.003 is used to update the prompts, and all experiments are conducted on a single NVIDIA 4090 GPU.

4.2. Comparison with State-of-the-arts

Compared methods. We compare our proposed SCAP with state-of-the-art TTA methods designed for CLIP adaptation, including TPT [36], C-TPT [47], DART [25], MTA [49], TDA [20], and Zero [7]. Additionally, we report

results from the original CLIP model to highlight the knowledge gained during testing. Following previous works [20], we also include training-time adaptation methods such as CoOp [57], CoCoOp [56], and Tip-Adapter [51] for comparison to further verify the label efficiency and effectiveness of our approach.

Results on the OOD Benchmark. As shown in Tab. 1, our proposed SCAP achieves state-of-the-art performance on the ImageNet-A, ImageNet-R, and ImageNet-S datasets, outperforming existing methods by at least **3.17%**, **1.44%**, and **1.11%**, respectively. Additionally, on the challenging ImageNet-V2 dataset, SCAP performs comparably to TDA, with only a marginal 0.02% difference. While TDA benefits from a feature cache to enable joint learning across multiple samples, it incurs additional storage overhead. In contrast, SCAP achieves comparable or superior performance without maintaining historical features, making it more efficient in practice.

Overall, SCAP improves average accuracy across the four ImageNet variants by **1.74%**, highlighting its effectiveness in handling natural object images across diverse distribution shifts. This performance gain is primarily attributed to the proposed supportive clique mining strategy, which ef-

Components in SCAP			ImageNet-A
Image	Text	Retention	Acc@1
✗	✗	✗	60.98
✗	✓	✗	62.57
✓	✗	✗	63.14
✓	✗	✓	63.82
✓	✓	✓	64.52

Table 2. Ablation study about the different components

- *Image* and *Text* represent learning from the Image Modality and Text Modality in the *Attribute Prompt Learning* module, respectively.
- *Retention* refers only to the *Retention Cache* for the visual modality while the *text retention prompts* are always used.

fectively captures diverse object attributes, such as “head” and “body”, that enhance the object recognition capacity of the model.

Results over cross-domain benchmark. As shown in Fig. 3, we compare our SCAP method with state-of-the-art approaches across four cross-domain datasets. The results demonstrate that our method surpasses the state-of-the-art approaches, with improvements of at least **1.64%**, **0.23%**, **0.18%**, and **0.24%** on the Pets, Flower102, Caltech101, and Aircraft datasets, respectively. This superior performance stems from the proposed Attribute Prompt Learning and Attribute Prompt Retention mechanisms, which effectively capture and leverage generalizable knowledge shared across diverse samples.

4.3. Ablation Studies

The Influence of Each Component. To evaluate the effectiveness of our module designs across different modalities (*i.e.*, image, text, and retention), we conduct modality-specific ablation studies. As shown in Tab. 2, leveraging both image and text modalities within the *Attribute Prompt Learning* module consistently improves performance over the baseline model. Additionally, incorporating the *Attribute Prompt Retention* module further enhances the utilization of learned image prompts, leading to substantial performance gains. Furthermore, when all modules and modalities are integrated, the model performance improves further due to joint optimization, which mitigates semantic drift as learnable parameters are updated.

The Influence of Batch Size in SCAP. Batch Size B is an important factor in the transductive TTA setting, as larger batches provide richer inter-image relationships. As illustrated in Fig. 4 (Left), the model performance consistently improves with increasing batch size, demonstrating SCAP’s capability to leverage the additional contextual information. We also observe that the image modality varies significantly as batch size changes, while the text modality remains relatively stable across batch size variations. On

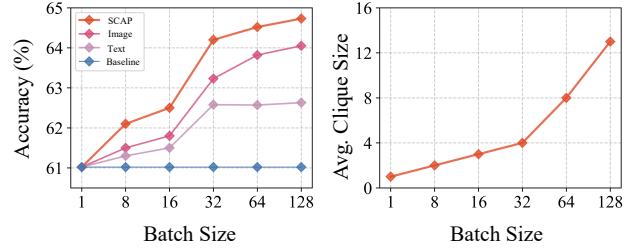


Figure 4. Left: the influence of batch size on SCAP performance. Right: the average maximum Clique size generated per batch under different batch sizes.

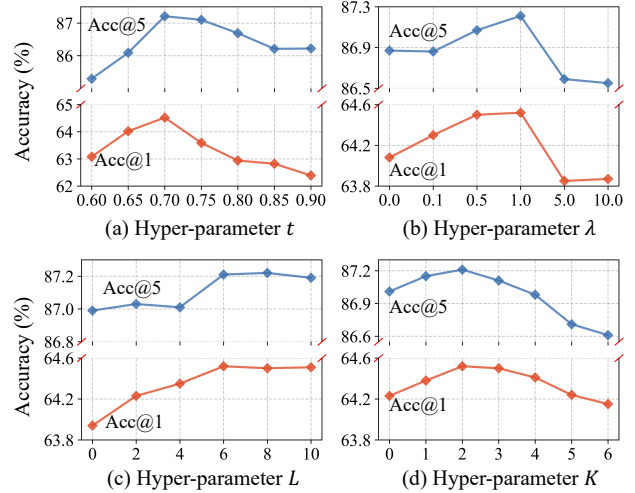


Figure 5. Ablation study about the influence of different hyperparameters on ImageNet-A.

the right side of Fig. 4, the results reveal that larger batches lead to increasing average clique size, indicating that more support information can be captured under such conditions.

The Influence of Different Hyperparameters. The key hyperparameters in our approach include the threshold t for clique extraction, the concentration loss weight λ , the retention cache limit L , and the degree of the retention graph K . As illustrated in Fig. 5 (a), the model performance is relatively sensitive to changes in t . A lower t results in cliques containing unrelated images, which hinders effective attribute prompt learning, whereas a higher t limits the number of support samples, leading to insufficient attribute modeling. Subsequently, we explore the impact of λ in Fig. 5 (b). The model performance improves consistently up to $\lambda = 1.0$, as the concentration loss enhances attribute learning. However, further increasing λ leads to overfitting, negatively affecting generalization. Then, we investigate the influence of L in Fig. 5 (c). We observe that as L increases, the performance increases and then becomes stable, indicating that while a larger cache enhances retention,

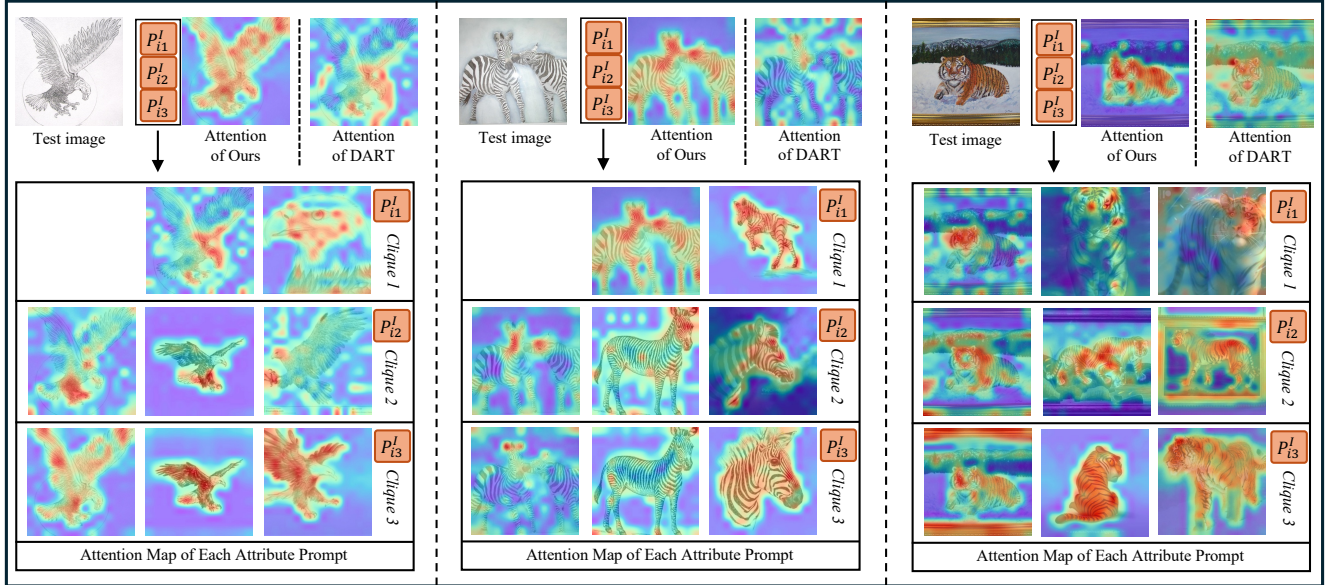


Figure 6. Visualization of our prompt-guided attention maps in comparison with the state-of-the-art prompt-based method.

Combine \mathcal{P}_{ik}^I		Combine P^I, P^{I*}		ImageNet-A
Mean	Concat	Mean	Concat	Acc@1
✓	✗	✓	✗	61.82
✓	✗	✗	✓	62.11
✗	✓	✓	✗	64.35
✗	✓	✗	✓	64.52

Table 3. The influence of different combination approaches.

excessive stored knowledge does not yield further gains. Finally, we study the influence of K in Fig. 5 (d). Increasing K up to 2 improves performance by strengthening graph connectivity and enhancing information propagation. However, beyond this point, performance declines due to the inclusion of irrelevant nodes, which introduces noise and reduces the discriminative power of the learned attributes.

Influence of Different Prompt Combination Approaches. Two primary strategies for combining multiple prompts are considered: generating a mean prompt and concatenating prompts along the token dimension, as illustrated in Eq. (15) and in Eq. (17). Experimental results in Table 3 indicate that concatenation outperforms averaging in our SCAP framework. This advantage due to concatenation preserves the full prompt information, enabling each prompt to focus on distinct image regions. In contrast, the mean prompt approach struggles to capture diverse visual patterns, leading to suboptimal performance.

Visualization of Supportive Cliques. To demonstrate the effectiveness of our supportive clique-based attribute prompt learning approach, we visualize the attention

maps in comparison with the state-of-the-art prompt-based method DART [25]. As illustrated in Fig. 6, each supportive clique in our method guides the prompts to focus on specific object parts, such as the head, leg, or body. When the attribute prompts are exploited together, the obtained attention maps precisely and comprehensively capture the object information, highlighting the superior feature-learning capability of our approach over DART.

5. Conclusion

In this paper, we propose a novel transductive test-time adaptation approach, Supportive Clique-based Attribute Prompting (SCAP), which leverages intrinsic cross-sample shared visual attributes to enhance model adaptation during testing. Specifically, our method identifies and models the attributes within batches through supportive cliques, sets of samples exhibiting similar patterns. Furthermore, a retention module is designed to dynamically store, aggregate, and utilize knowledge from previously learned attributes, thereby improving predictions for subsequent test images. Extensive experiments on two benchmarks demonstrate the effectiveness of our method in leveraging batch-wise information. The proposed approach offers a promising direction for fully exploiting cross-sample relationships in practical transductive TTA scenarios.

Acknowledgments. This work was supported by the grants from the National Natural Science Foundation of China (62376011, 61925201, 62132001, 62432001) and Beijing Natural Science Foundation (L247006).

References

- [1] Malik Boudiaf, Romain Mueller, Ismail Ben Ayed, and Luca Bertinetto. Parameter-free online test-time adaptation. In *CVPR*, pages 8344–8353, 2022. 2
- [2] Dian Chen, Dequan Wang, Trevor Darrell, and Sayna Ebrahimi. Contrastive test-time adaptation. In *CVPR*, pages 295–305, 2022. 2
- [3] Zhenyu Cui, Yuxin Peng, Xun Wang, Manyu Zhu, and Jiahuan Zhou. Continual vision-language retrieval via dynamic knowledge rectification. In *AAAI*, pages 11704–11712, 2024. 2
- [4] Jia Deng, Wei Dong, Richard Socher, Li-Jia Li, Kai Li, and Li Fei-Fei. Imagenet: A large-scale hierarchical image database. In *CVPR*, pages 248–255. Ieee, 2009. 5
- [5] Karan Desai and Justin Johnson. Virtex: Learning visual representations from textual annotations. In *CVPR*, pages 11162–11173, 2021. 2
- [6] Mario Döbler, Robert A Marsden, and Bin Yang. Robust mean teacher for continual and gradual test-time adaptation. In *CVPR*, pages 7704–7714, 2023. 2
- [7] Matteo Farina, Gianni Franchi, Giovanni Iacca, Massimiliano Mancini, Elisa Ricci, et al. Frustratingly easy test-time adaptation of vision-language models. In *NeurIPS*, 2024. 1, 2, 6
- [8] Li Fei-Fei, Rob Fergus, and Pietro Perona. Learning generative visual models from few training examples: An incremental bayesian approach tested on 101 object categories. In *CVPRW*, pages 178–178. IEEE, 2004. 5
- [9] Chun-Mei Feng, Kai Yu, Yong Liu, Salman Khan, and Wangmeng Zuo. Diverse data augmentation with diffusions for effective test-time prompt tuning. In *ICCV*, pages 2704–2714, 2023. 2
- [10] Lihua Fu, Yubin Du, Yu Ding, Dan Wang, Hanxu Jiang, and Haitao Zhang. Domain adaptive learning with multi-granularity features for unsupervised person re-identification. *Chinese Journal of Electronics*, 31(1):116–128, 2022. 2
- [11] Yulu Gan, Yan Bai, Yihang Lou, Xianzheng Ma, Renrui Zhang, Nian Shi, and Lin Luo. Decorate the newcomers: Visual domain prompt for continual test time adaptation. In *AAAI*, pages 7595–7603, 2023. 2
- [12] Yulu Gan, Yan Bai, Yihang Lou, Xianzheng Ma, Renrui Zhang, Nian Shi, and Lin Luo. Decorate the newcomers: Visual domain prompt for continual test time adaptation. In *AAAI*, pages 7595–7603, 2023. 3
- [13] Taesik Gong, Yewon Kim, Taeckyoung Lee, Sorn Chottanurak, and Sung-Ju Lee. Sotta: Robust test-time adaptation on noisy data streams. *NeurIPS*, 36, 2024. 2, 3
- [14] Gustavo Adolfo Vargas Hakim, David Osowiechi, Mehrdad Noori, Milad Cheraghalikhani, Ali Bahri, Moslem Yazdanpanah, Ismail Ben Ayed, and Christian Desrosiers. Clipartt: Light-weight adaptation of clip to new domains at test time. *arXiv preprint arXiv:2405.00754*, 2024. 2, 3
- [15] Dan Hendrycks, Steven Basart, Norman Mu, Saurav Kadavath, Frank Wang, Evan Dorundo, Rahul Desai, Tyler Zhu, Samyak Parajuli, Mike Guo, et al. The many faces of robustness: A critical analysis of out-of-distribution generalization. In *ICCV*, pages 8340–8349, 2021. 5
- [16] Dan Hendrycks, Kevin Zhao, Steven Basart, Jacob Steinhardt, and Dawn Song. Natural adversarial examples. In *CVPR*, pages 15262–15271, 2021. 5
- [17] Xuefeng Hu, Gokhan Uzunbas, Sirius Chen, Rui Wang, Ashish Shah, Ram Nevatia, and Ser-Nam Lim. Mixnorm: Test-time adaptation through online normalization estimation. *arXiv preprint arXiv:2110.11478*, 2021. 2
- [18] Xiaowei Hu, Zhe Gan, Jianfeng Wang, Zhengyuan Yang, Zicheng Liu, Yumao Lu, and Lijuan Wang. Scaling up vision-language pre-training for image captioning. In *CVPR*, pages 17980–17989, 2022. 2
- [19] Chao Jia, Yinfei Yang, Ye Xia, Yi-Ting Chen, Zarana Parekh, Hieu Pham, Quoc Le, Yun-Hsuan Sung, Zhen Li, and Tom Duerig. Scaling up visual and vision-language representation learning with noisy text supervision. In *ICML*, pages 4904–4916. PMLR, 2021. 2
- [20] Adilbek Karmanov, Dayan Guan, Shijian Lu, Abdulmotaleb El Saddik, and Eric Xing. Efficient test-time adaptation of vision-language models. In *CVPR*, pages 14162–14171, 2024. 1, 2, 6
- [21] Muhammad Uzair Khattak, Hanoona Rasheed, Muhammad Maaz, Salman Khan, and Fahad Shahbaz Khan. Maple: Multi-modal prompt learning. In *CVPR*, pages 19113–19122, 2023. 2
- [22] Qiwei Li, Kunlun Xu, Yuxin Peng, and Jiahuan Zhou. Exemplar-free lifelong person re-identification via prompt-guided adaptive knowledge consolidation. *IJCV*, 132(11): 4850–4865, 2024. 2
- [23] Xin Li, Dongze Lian, Zhihe Lu, Jiawang Bai, Zhibo Chen, and Xinchao Wang. Graphadapter: Tuning vision-language models with dual knowledge graph. *NeurIPS*, 36:13448–13466, 2023. 2
- [24] Zichen Liu, Yuxin Peng, and Jiahuan Zhou. Insvp: Efficient instance visual prompting from image itself. In *Proceedings of the 32nd ACM International Conference on Multimedia*, pages 6443–6452, 2024. 2
- [25] Zichen Liu, Hongbo Sun, Yuxin Peng, and Jiahuan Zhou. Dart: dual-modal adaptive online prompting and knowledge retention for test-time adaptation. In *AAAI*, pages 14106–14114, 2024. 1, 2, 3, 6, 8
- [26] Xiaosong Ma, Jie Zhang, Song Guo, and Wenchao Xu. Swapprompt: Test-time prompt adaptation for vision-language models. *NeurIPS*, 36, 2024. 3
- [27] Subhransu Maji, Esa Rahtu, Juho Kannala, Matthew Blaschko, and Andrea Vedaldi. Fine-grained visual classification of aircraft. *arXiv preprint arXiv:1306.5151*, 2013. 5
- [28] Robert A Marsden, Mario Döbler, and Bin Yang. Universal test-time adaptation through weight ensembling, diversity weighting, and prior correction. In *WACV*, pages 2555–2565, 2024. 2, 3
- [29] Maria-Elena Nilsback and Andrew Zisserman. Automated flower classification over a large number of classes. In *2008 Sixth Indian conference on computer vision, graphics & image processing*, pages 722–729. IEEE, 2008. 5

- [30] Omkar M Parkhi, Andrea Vedaldi, Andrew Zisserman, and CV Jawahar. Cats and dogs. In *CVPR*, pages 3498–3505. IEEE, 2012. 5
- [31] Ori Press, Steffen Schneider, Matthias Kümmerer, and Matthias Bethge. Rdumb: A simple approach that questions our progress in continual test-time adaptation. *NeurIPS*, 36: 39915–39935, 2023. 2, 3
- [32] Alec Radford, Jong Wook Kim, Chris Hallacy, Aditya Ramesh, Gabriel Goh, Sandhini Agarwal, Girish Sastry, Amanda Askell, Pamela Mishkin, Jack Clark, et al. Learning transferable visual models from natural language supervision. In *ICML*, pages 8748–8763. PMLR, 2021. 1, 2, 6
- [33] Alec Radford, Jong Wook Kim, Chris Hallacy, Aditya Ramesh, Gabriel Goh, Sandhini Agarwal, Girish Sastry, Amanda Askell, Pamela Mishkin, Jack Clark, et al. Learning transferable visual models from natural language supervision. In *ICML*, pages 8748–8763. PmLR, 2021. 2
- [34] Benjamin Recht, Rebecca Roelofs, Ludwig Schmidt, and Vaishaal Shankar. Do imagenet classifiers generalize to imagenet? In *ICML*, pages 5389–5400. PMLR, 2019. 5
- [35] Steffen Schneider, Evgenia Rusak, Luisa Eck, Oliver Bringmann, Wieland Brendel, and Matthias Bethge. Improving robustness against common corruptions by covariate shift adaptation. *NeurIPS*, 33:11539–11551, 2020. 3
- [36] Manli Shu, Weili Nie, De-An Huang, Zhiding Yu, Tom Goldstein, Anima Anandkumar, and Chaowei Xiao. Test-time prompt tuning for zero-shot generalization in vision-language models. *NeurIPS*, 35:14274–14289, 2022. 2, 3, 6
- [37] Junha Song, Jungsoo Lee, In So Kweon, and Sungha Choi. Ecotta: Memory-efficient continual test-time adaptation via self-distilled regularization. In *CVPR*, pages 11920–11929, 2023. 2
- [38] Dequan Wang, Evan Shelhamer, Shaoteng Liu, Bruno Olshausen, and Trevor Darrell. Tent: Fully test-time adaptation by entropy minimization. In *ICLR*. 2, 3
- [39] Dequan Wang, Evan Shelhamer, Shaoteng Liu, Bruno Olshausen, and Trevor Darrell. Tent: Fully test-time adaptation by entropy minimization. *arXiv preprint arXiv:2006.10726*, 2020. 2, 3
- [40] Haohan Wang, Songwei Ge, Zachary Lipton, and Eric P Xing. Learning robust global representations by penalizing local predictive power. *NeurIPS*, 32, 2019. 5
- [41] Qin Wang, Olga Fink, Luc Van Gool, and Dengxin Dai. Continual test-time domain adaptation. In *CVPR*, pages 7201–7211, 2022. 3
- [42] Kunlun Xu, Haozhuo Zhang, Yu Li, Yuxin Peng, and Jiahuan Zhou. Mitigate catastrophic remembering via continual knowledge purification for noisy lifelong person re-identification. In *ACM MM*, pages 5790–5799, 2024. 2
- [43] Kunlun Xu, Xu Zou, Yuxin Peng, and Jiahuan Zhou. Distribution-aware knowledge prototyping for non-exemplar lifelong person re-identification. In *CVPR*, pages 16604–16613, 2024. 1
- [44] Kunlun Xu, Xu Zou, and Jiahuan Zhou. Lstkc: Long short-term knowledge consolidation for lifelong person re-identification. In *AAAI*, pages 16202–16210, 2024. 2
- [45] Jinyu Yang, Jiali Duan, Son Tran, Yi Xu, Sampath Chanda, Liquan Chen, Belinda Zeng, Trishul Chilimbi, and Junzhou Huang. Vision-language pre-training with triple contrastive learning. In *CVPR*, pages 15671–15680, 2022. 2
- [46] Zhaoda Ye, Xiangteng He, and Yuxin Peng. Unsupervised cross-media hashing learning via knowledge graph. *Chinese Journal of Electronics*, 31(6):1081–1091, 2022. 1
- [47] Hee Suk Yoon, Eunseop Yoon, Joshua Tian Jin Tee, Mark Hasegawa-Johnson, Yingzhen Li, and Chang D Yoo. C-tp: Calibrated test-time prompt tuning for vision-language models via text feature dispersion. *arXiv preprint arXiv:2403.14119*, 2024. 3, 6
- [48] Tao Yu, Zhihe Lu, Xin Jin, Zhibo Chen, and Xinchao Wang. Task residual for tuning vision-language models. In *CVPR*, pages 10899–10909, 2023. 2
- [49] Maxime Zanella and Ismail Ben Ayed. On the test-time zero-shot generalization of vision-language models: Do we really need prompt learning? In *CVPR*, pages 23783–23793, 2024. 2, 6
- [50] Ding-Chu Zhang, Zhi Zhou, and Yu-Feng Li. Robust test-time adaptation for zero-shot prompt tuning. In *AAAI*, pages 16714–16722, 2024. 2, 3
- [51] Renrui Zhang, Wei Zhang, Rongyao Fang, Peng Gao, Kunchang Li, Jifeng Dai, Yu Qiao, and Hongsheng Li. Tip-adapter: Training-free adaption of clip for few-shot classification. In *ECCV*, pages 493–510. Springer, 2022. 2, 6
- [52] Ruru Zhang, E Haihong, and Meina Song. Fscil-eaca: Few-shot class-incremental learning network based on embedding augmentation and classifier adaptation for image classification. *Chinese Journal of Electronics*, 33(1):139–152, 2024. 1
- [53] Dengyong Zhou, Olivier Bousquet, Thomas Lal, Jason Weston, and Bernhard Schölkopf. Learning with local and global consistency. *NeurIPS*, 16, 2003. 5
- [54] Jiahuan Zhou, Pei Yu, Wei Tang, and Ying Wu. Efficient online local metric adaptation via negative samples for person re-identification. In *ICCV*, pages 2420–2428, 2017. 2
- [55] Jiahuan Zhou, Bing Su, and Ying Wu. Online joint multi-metric adaptation from frequent sharing-subset mining for person re-identification. In *CVPR*, pages 2909–2918, 2020. 1
- [56] Kaiyang Zhou, Jingkang Yang, Chen Change Loy, and Ziwei Liu. Conditional prompt learning for vision-language models. In *CVPR*, pages 16816–16825, 2022. 2, 6
- [57] Kaiyang Zhou, Jingkang Yang, Chen Change Loy, and Ziwei Liu. Learning to prompt for vision-language models. *IJCV*, 130(9):2337–2348, 2022. 2, 6

SCAP: Transductive Test-Time Adaptation via Supportive Clique-based Attribute Prompting

Supplementary Material

1. Benchmark Details

Here, we provide the sub-dataset details of the out-of-distribution (OOD) and cross-domain benchmarks exploited in this paper.

1.1. Details on Datasets in the OOD Benchmark

Our OOD benchmark consists of four out-of-distribution datasets derived from ImageNet [?].

- **ImageNet-A** [?] contains 7,500 images of 200 classes that are naturally perturbed and misclassified by ResNet-50 [?] in ImageNet.
- **ImageNet-R** [?] includes 30,000 images covering 200 classes across 16 artistic and stylistic domains, such as cartoons, graffiti, and sketches, posing significant challenges due to their diverse visual transformations.
- **ImageNet-Sketch** [?] contains 50,000 images of 1,000 categories. The distribution of ImageNet-Sketch differs greatly from the pre-training data of CLIP since it only contains black-and-white sketches. Thus, it has been a challenging dataset for TTA.
- **ImageNet-V2** [?] comprises 10,000 images across 1,000 classes, sampled a decade after the original ImageNet dataset. It presents a naturally evolved distribution shift, making it a realistic benchmark for evaluating generalization performance..

OOD Datasets	Size	Number of Classes
ImageNet-A	7,500	200
ImageNet-R	30,000	200
ImageNet-Sketch	50,000	1,000
ImageNet-V2	10,000	1,000

Table 1. Overview of datasets in OOD benchmark

Cross-Domain	Size	Number of Classes
Aircraft	3,333	100
Caltech101	2,465	100
Flower102	2,463	102
Pets	3,669	37

Table 2. Overview of datasets in Cross-domain benchmark.

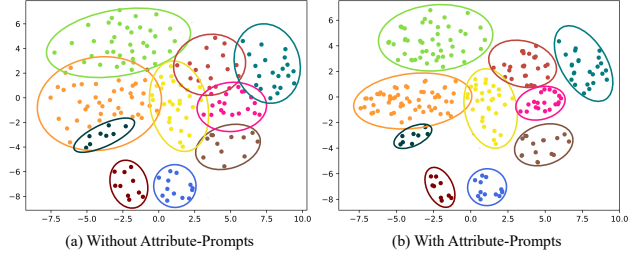


Figure 1. Visualization of the distribution of image features with and without the learned Attribute Prompts.

1.2. Details on Datasets in Cross-domain Benchmark

The cross-domain benchmark comprises four datasets from distinct visual domains, providing a diverse evaluation setting for assessing model generalization.

- **Aircraft** [?] consists of 10,200 images representing 102 different aircraft model variants, each with 100 images. The dataset predominantly features airplanes and poses challenges in fine-grained visual classification.
- **Caltech101** [?] includes 2,465 images spanning 101 object categories along with a background class. Each category contains 40 to 800 images, with most classes averaging around 50 samples, making it a benchmark for object recognition tasks.
- **Flower102** [?] comprises 2,463 images of 102 flower species. Due to the significant domain gap between flowers and standard pretraining datasets, this dataset serves as a robust test for domain generalization.
- **Pets** [?] contains images of cats and dogs across 37 different breeds. The dataset exhibits high intra-class variations in scale, pose, and lighting, making it challenging for fine-grained classification tasks.

2. The Effectiveness of Attribute Prompts

To demonstrate the effectiveness of our supportive clique-based attribute prompting, we visualize the embedding distributions of images from different classes in Figure 1, where with and without the corresponding Attribute Prompts setting are conducted. As illustrated in Figure 1, incorporating Attribute Prompts improves intra-class compactness and inter-class discrimination. Notably, several previously ambiguous samples near class boundaries shift closer to their respective class centers, thereby enhancing the overall quality of the learned image representations.

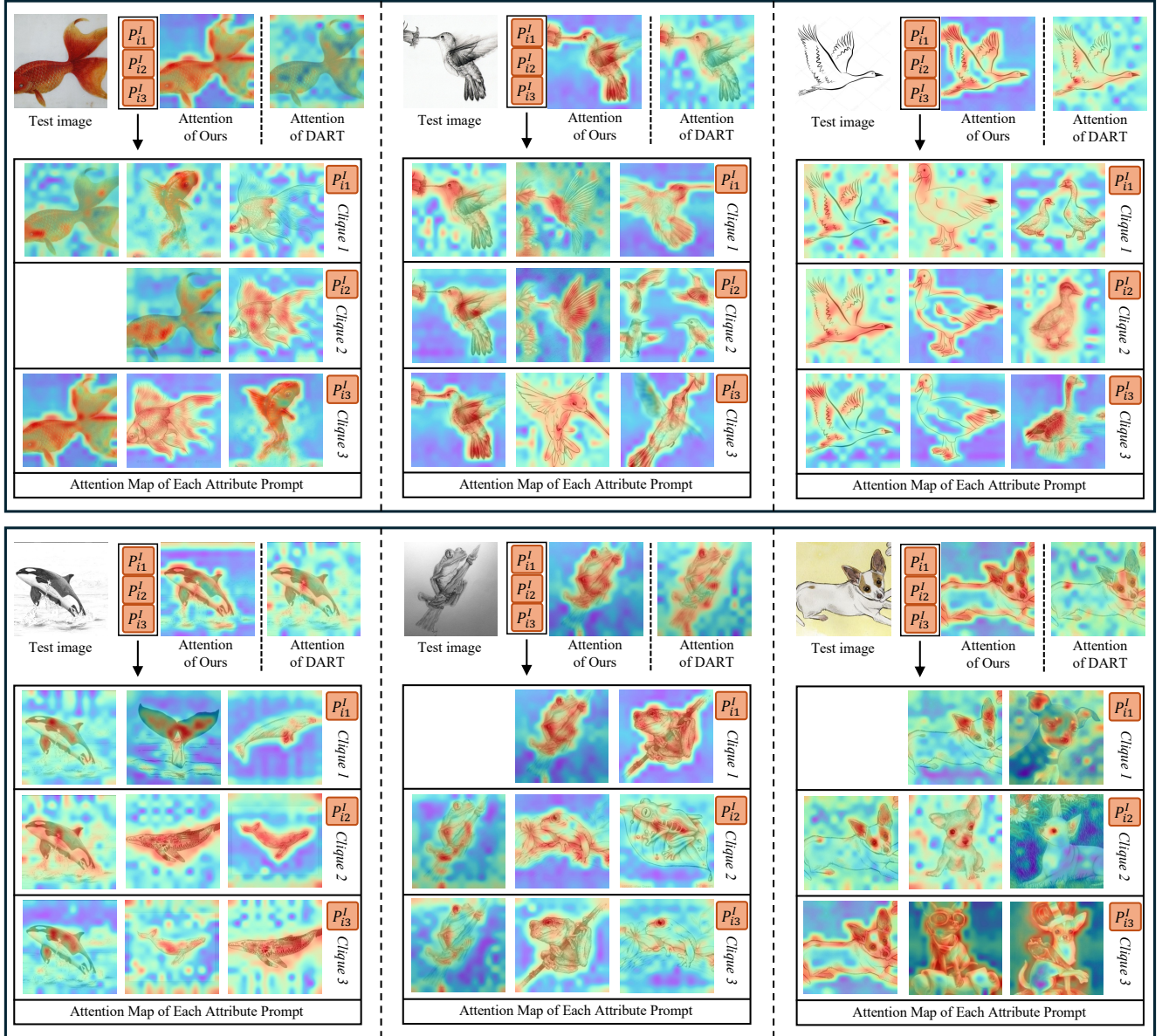


Figure 2. Additional visualization results of the attention maps.

Method	Publication	Cars	SUN397	Aircraft	EuroSAT	Food101	Pets	Flower102	Caltech101	DTD	UCF101	Average
TDA	CVPR 2024	67.28	67.62	23.91	58.00	86.14	88.63	71.42	94.24	47.40	70.66	67.53
SCAP	This Paper	69.25	66.41	25.44	58.62	86.58	90.27	71.65	94.42	47.79	68.36	67.88

Table 3. Additional Results on the domain-shift datasets. SCAP compared with the second-highest TDA.

This improvement is attributed to our proposed *Concentration Loss*, which, together with *Entropy Loss*, encourages samples within the same supportive clique to leverage shared attributes, leading to more tightly clustered and semantically consistent features.

3. Visualization of Attention Maps

In Fig. 2, we provide additional visualizations of the attention maps in comparison with DART [?]. The results demonstrate that each of our *visual attribute prompts* guides CLIP to attend to the specific attributes shared among

images within a supportive clique, thereby enabling fine-grained attribute-based prompt learning. By aggregating all relevant *visual attribute prompts* associated with a given test image, our approach effectively directs attention toward the most salient attributes, leading to enhanced feature extraction and improved classification performance. In contrast, the attention maps generated by DART often exhibit dispersed or incomplete attention, failing to sufficiently capture critical object attributes. These findings highlight the superior prompt-learning capability of SCAP in accurately and comprehensively leveraging visual information.

4. Additional Results on the domain-shift datasets

In Tab. 3, we report results on six additional datasets alongside the four datasets in our main paper from the cross-domain benchmark. SCAP consistently outperforms the second-best method, TDA, on eight out of ten datasets, achieving an average accuracy improvement of **0.35%**. These results further demonstrate SCAP’s effectiveness in adapting to diverse domain shifts, highlighting its robustness in transductive TTA scenarios.